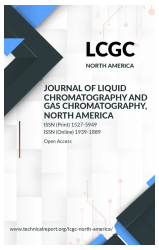

Journal of Liquid Chromatography and Gas Chromatography, North America
https://technicalreport.org/lcgcnam

LC GC N. Am., Vol. 42, No.1, 09-13, 2024

Technical Reports Press

RESEARCH ARTICLE

Endogenous-Blank Partitioning of Serum miR-18a Recovery on a Nanoporous-Gold Y-Shaped Electrochemical Biosensor

Simon Bott[1*]

[1] *College of Natural Sciences and Mathematics, University of Houston, Houston, TX, USA*
[*] *Corresponding author*

Corresponding author:
s.g.bott@swansea.ac.uk

Received: 23 November 2025
Accepted: 23 November 2025
Available online: 23 November 2025

Abstract
The precise determination of serum microRNA entails clear distinction between the presence of endogenous target in biological samples before spike recovery and the actual concentration delivered through spike additions. Here we propose an endogenous blank partitioning approach for the determination of serum miR-18a in terms of the nanoporous-gold Y-shaped electrochemical biosensing method. The fundamental issue is if three spiked levels of serum human targets can be translated into blank contribution, target recovery, concentration bias, and repeatability measures. The experimental record features three additional concentrations of miR-18a of 100 fmol L^{-1}, 1 pmol L^{-1}, and 10 pmol L^{-1}, combined with a serum blank of tenfold dilution, namely 24.165 fmol L^{-1}. Upon subtracting the blank concentration, the obtained values became 95.415 fmol L^{-1}, 1034.945 fmol L^{-1}, and 10480.525 fmol L^{-1}. Correspondingly, the percentage recoveries were estimated as 95.41%, 103.49%, and 104.81%, while the relative standard deviations were 1.81%, 2.19%, and 4.01%. Blank contributions accounted for 24.17% of the added concentration and 20.21% of the measured amount in case of the lowest level, whereas for the two higher levels they were reduced to 2.42% / 2.28% and 0.24% / 0.23%, respectively.

Keywords: miR-18a; serum microRNA; endogenous blank; nanoporous gold; electrochemical biosensor; recovery; non-small cell lung cancer

1. Introduction

Measurement of lung cancer by liquid biopsy analysis is an important trend in measurement science due to the potential of accessing blood-based molecular markers through minimally invasive procedures and using these measures as complements to radiology, tissue biopsy, and histopathology. MicroRNAs in this context are valuable because they are short RNAs capable of regulating genes on post-transcriptional levels and detectable in serum, plasma, vesicular fractions, and other body fluids. Biological significance in non-small cell lung cancer (NSCLC) combined with resistance to distortion by matrix contribution, sequence similarity, dilution factors, and recovery rates is the basis of the usefulness of circulating microRNAs [1–3].

Clinical translation of miRNA signatures in blood is hindered by pre-analytical variability, sample-type dependence, normalization, and lack of comparability between different cohorts. This means that in the case of miRNA concentration in the serum, the measurement involves several steps of sample treatment and signal generation which, combined with a biological signal itself, lead to the final result. Measurement reliability therefore becomes crucial, since it determines the ability to obtain low-concentration signals amidst protein and other serum matrixes and background miRNA levels [4–6].

A suitable example in this context is miR-18a. It is part of the miR-17-92 gene cluster and connected to various aspects of malignancy development and treatment [7–9]. From a biomarker perspective, it has been shown to have both diagnostic and prognostic relevance in NSCLC-oriented investigations, and the expression mechanisms of miR-18a have been connected to its ability to determine response to therapy in lung cancer [10, 11]. The technical difficulty of its measurement arises from the close relation of miR-18a to miR-18b,

Cite as: S. Bott (2024). Endogenous-Blank Partitioning of Serum miR-18a Recovery on a Nanoporous-Gold Y-Shaped Electrochemical Biosensor. LC GC N. Am., 42(1) (2024) 09-13.

which means that a successful miR-18a biosensor must be both highly sensitive and discriminative enough to recognize the sequence.
Electrochemical microRNA biosensors are a good choice in this context because of the possibility to implement molecular recognition and electrochemical signal generation in a compact and affordable design. Existing examples of microRNA electroanalysis include labelled probes, target displacement reactions, enzymatic amplification, nanoelectrodes, and ratiometric detection schemes [12–14]. However, high sensitivity is necessary but not sufficient for the reliable detection of miR-18a in the serum. Sample handling, probe immobilization, surface accessibility, and concentration conversion must all work together to provide an accurate final result [15–17]. As a consequence, a good biosensor design must not be seen as an electrode, but as an entire analytical system from serum to concentration.
Nanoporous gold is advantageous as a base material for an electrochemical biosensor because of its high surface conductivity, large available area, good chemical stability, and probe attachment via gold-thiol interactions. Its ligament-like porous structure may increase the surface load and facilitate interfacial electron transfer, though probe density and matrix interactions may restrict target accessibility. It is thus important to consider not the high surface area of nanoporous gold alone, but whether the final sensor will be able to reliably measure miR-18a in the serum.
The serum miR-18a recovery data provided by a Y-shaped electrochemical ratiometric biosensor based on nanoporous gold allows measuring the miR-18a concentration in femtomolar-to-picomolar ranges with discrimination against miR-18b [18]. Apart from their general importance, the numeric values also contain information about the relative influence of blank and spiked concentrations. For example, despite having an equal absolute value of 24.165 fmol L^{-1}, the blank represents 24.17% of a 100 fmol L^{-1} addition but only 2.42% of 1 pmol L^{-1} addition. This means that blanket statements on recovery should not hide concentration-related biases.
The research problem considered in the current report focuses specifically on this issue: can serum-spiked miR-18a values be partitioned into the endogenous serum blank contribution and recovered spiked concentration for independent evaluation of both parameters? In order to solve the problem, serum recovery data was decomposed into blank-corrected concentration, signed bias, blank burden, blank fraction, and recovery direction. This is a measurement interpretation study focusing on serum recovery and using existing experimental data, and not a new patient classifier or electrode design. The value of the analysis is in providing an interpretable way to read the provided serum spike values.

2. Materials and Methods

2.1. Analytical record and scope

Data processing uses human-serum recovery measurements conducted with the nanoporous-gold Y-shaped electrochemical miR-18a biosensor. The record includes three spiked concentrations (100 fmol L^{-1}, 1 pmol L^{-1}, and 10 pmol L^{-1}), three post-spike measured concentrations (119.58 fmol L^{-1}, 1059.11 fmol L^{-1}, and 10504.69 fmol L^{-1}), one tenfold diluted serum blank (24.165 fmol L^{-1}), recovery percentages, and relative standard deviations (1.81%, 2.19%, and 4.01%, respectively).
It is important to highlight the narrow scope of the analysis which includes only serum recovery, blank influence, concentration measurement, and repeatability. In other words, no new patient classifier or biosensor design experiment was included in the current investigation. The value of the current work therefore consists of converting provided numbers into concentration values and interpreting the resulting blank-related data. The purpose of the analysis is to explain why the same blank has different impacts at femtomolar and picomolar concentration values.

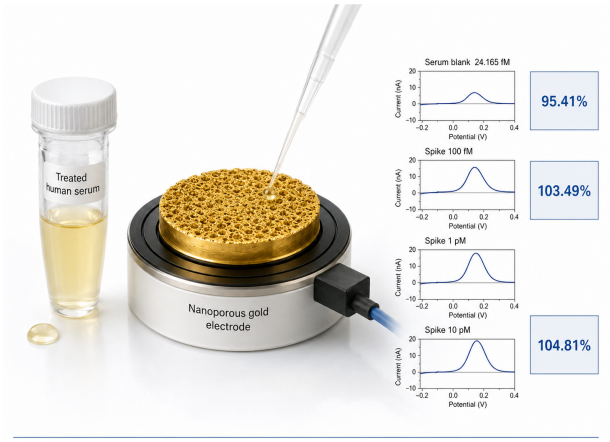

Figure 1: Serum-to-electrode workflow.

Workflow illustration shows the boundaries of analytical measurement in this report. Treated serum with added miR-18a is provided to the prepared nanoporous gold electrode, the target is detected and hybridized to the probes arranged on the biosensor, and the electrochemical signal provides the total concentration measurement. The total concentration is not a result of spiked miR-18a alone because of endogenous miR-18a in the matrix. It must therefore be corrected for blank before further analysis.

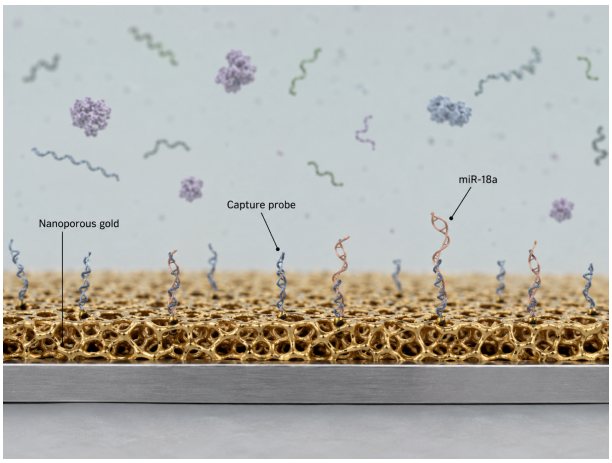

Figure 2: Nanoporous-gold sensing interface.

Sensor illustration specifies the basic materials and molecular interaction involved in the measurement. Nanoporous gold provides a high-conductivity surface area for thiolated probe immobilization, and a Y-shaped probe arrangement allows discriminating miR-18a from miR-18b and generating a ratiometric electrochemical signal. Concentration analysis begins after signal generation and asks the question of whether the obtained value is affected by the endogenous blank in the serum.

2.2. Blank partitioning and calculations

Blank partitioning involves splitting the total value into two parts: the endogenous blank measured in the treated serum and the added miR-18a recovered from the spike addition. Blank-corrected concentration was obtained by subtracting 24.165 fmol L^{-1} from the total concentration value. Recovery was computed by dividing the blank-corrected value by the spiked concentration and converting to percentage. Signed bias was obtained by subtracting the spiked value from the blank-corrected value.

Two additional terms were introduced to facilitate interpretation. Blank burden is the relative share of serum blank in the spiked concentration, and blank fraction is the relative share of the blank in the total concentration value. They differentiate the low-concentration situation where blank correction has high impact from high-concentration situation where blank contribution to total concentration is insignificant.

2.3. Decision criteria

A concentration level was defined as acceptable when the blank-corrected recovery was in the range of 95-105% and the relative standard deviation was below 5%. Since a single average recovery is not informative about concentration-specific weaknesses, each individual level had to meet the above criteria to be described as such.

3. Results and Discussion

3.1. Endogenous blank as a concentration-dependent factor

As mentioned above, blank was constant, but its effect on concentration changed drastically with the changing spiked concentration values. Specifically, the blank constituted 24.17% of the lowest addition but only 2.42% of the first picomolar addition, and 0.24% of the second picomolar addition. Such a pronounced difference between concentration ranges is an indication of separate evaluation.

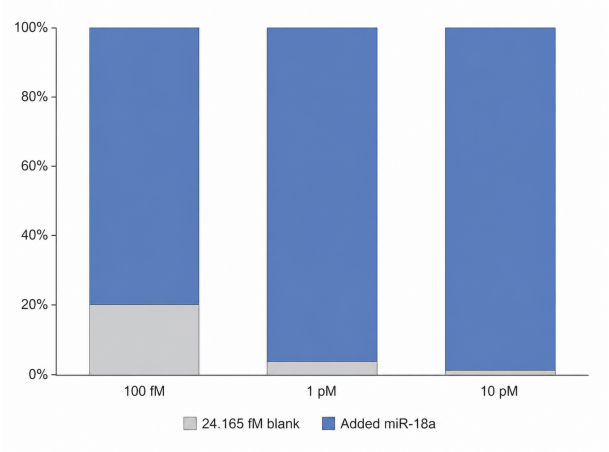

Figure 3: Serum blank burden.

This fact is reflected in the serum blank burden graph. An 24.165 fmol L^{-1} blank constitutes a significant part of the lowest concentration addition, but only a small proportion of picomolar concentrations. In other words, the 100 fmol L^{-1} concentration level is best regarded as a blank-related analysis tool, while picomolar levels are better understood as high concentration analysis tasks.

Table 1: Blank-partitioned serum miR-18a values.

Matrix	Added	Measured	Blank	Corrected	Recovery	RSD
		(fmol L^{-1})			(%)	(%)
Human serum	100	119.58	24.165	95.415	95.41	1.81
Human serum	1000	1059.11	24.165	1034.945	103.49	2.19
Human serum	10000	10504.69	24.165	10480.525	104.81	4.01

Partitioning reveals that all adjusted concentrations lie very close to the known additions; however, analytical interpretation differs at each level. The minimum spiked value falls below the threshold of recovery range only with careful blank subtraction. The medium-level value possesses minimal contribution of blank, moderately good positive recovery, and excellent reproducibility. The maximal spiked value lies within the acceptance criteria but demonstrates the maximum relative standard deviation and the maximal positive bias in signed form.

Added (fM)	Measured (fM)	Blank (fM)	Corrected (fM)
100	119.58	24.165	95.415
1000	1059.11	24.165	1034.945
10000	10504.69	24.165	10480.525

Figure 4: Recovery value structure.

The recovery-structure graph emphasizes the difference between total concentration and amount of added miR-18a. It should be noted that the analytical relevance arises only following the subtraction of the fixed serum blank value. This point is significant in serum microRNA quantitation since a sample with low concentration can be interpreted positively for total concentration but negatively for correction-based recovery.

3.2. Recovery bias and acceptance corridor

The blank-corrected recoveries lay between 95.41 % and 104.81 %. All these values fell into the 95%–105% acceptance corridor, but the bias direction varied along the concentration spectrum. The femtomolar level had signed bias equal to -4.585 fmol L^{-1}; the picomolar level demonstrated signed bias equal to 34.945 fmol L^{-1}; and the 10-picomolar level had signed bias 480.525 fmol L^{-1}. The change in bias direction with increasing levels testifies to concentration-related behaviour.

Table 2: Blank burden and signed bias.

Added (fmol L^{-1})	Signed bias (fmol L^{-1})	Blank burden (%)	Blank fraction (%)	Recovery direction	Decision
100	-4.585	24.17	20.21	Below reference	Accepted, blank-sensitive
1000	34.945	2.42	2.28	Above reference	Accepted, stable transfer
10000	480.525	0.24	0.23	Above reference	Accepted, upper-near

The most direct answer comes from the descriptor table itself, distinguishing between endogenous serum contribution and concentration transfer in the context of blank correction. While the 100 fmol L^{-1} spike concentration is the only point at which the blank dominates interpretive caution, the 1 pmol L^{-1} spike concentration is the most stable point in terms of minimal blank burden and high repeatability. In contrast, the 10 pmol L^{-1} spike concentration is acceptable but upper-bound-near due to elevated recovery, signed bias, and relative standard deviation.

The recovery acceptance corridor graph demonstrates that all tested serum-spiking concentrations pass the selected criterion. It also makes a deeper point about acceptance: that is does not equal identical analytical behaviour. On one hand, the lowest concentration spikes lie close to the bottom of the acceptance corridor while the highest concentration spikes lie near the top. Reporting only the mean recovery hides this directionality.

3.3. Concentration transfer across femtomolar and picomolar levels

The concentration transfer analysis demonstrates a near-proportional behaviour over a one-hundred-fold interval. Corrected concentrations

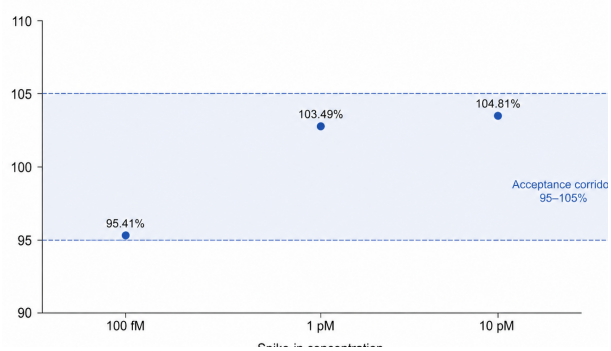

Figure 5: Recovery acceptance corridor.

were 95.415 fmol L^{-1}, 1034.945 fmol L^{-1}, and 10480.525 fmol L^{-1}. The lower concentration indicates the feasibility of low-femtomolar quantification after blank subtraction, though this result is highly blank-sensitive. The middle concentration is consistent with stable concentration transfer around 1 pmol L^{-1}. Finally, the upper concentration confirms successful signal recovery at 10 pmol L^{-1} with positive signed bias in the acceptable corridor.

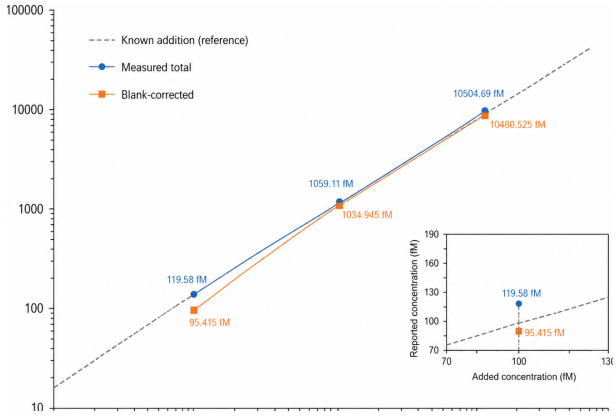

Figure 6: Concentration transfer.

The concentration transfer plot supports the main analytical conclusion. The total measured concentrations are consistently larger than blank-corrected concentrations due to endogenous serum contribution to the total signal. The effect was most visible in the lowest spike concentration while the highest spike concentrations demonstrated almost parallel lines in terms of their proximity. Such behaviour supports the need to separate the blank signal from the added concentration.

3.4. Precision and repeatability

While both recovery and repeatability serve the purpose of ensuring analytical validity, they measure fundamentally different aspects of it. Recovery indicates closeness to known addition after subtracting blank signal. Relative standard deviation, on the other hand, measures replicability, i.e., closeness of measurements to each other. The obtained relative standard deviations were 1.81%, 2.19%, and 4.01%, all falling under the acceptable 5% limit, indicating acceptable repetitiveness of the biosensor response.

While the precision graph prevents misinterpreting recovery results, it also reveals important details about the process. For example, despite being blank-sensitive, the smallest spike concentration was not the least repetitive. Instead, the highest concentration displayed the largest relative standard deviation, though still remaining acceptable. Such information helps make a well-informed analytical conclusion – the key limiting factor in the lowest spike concentration is blank contribution

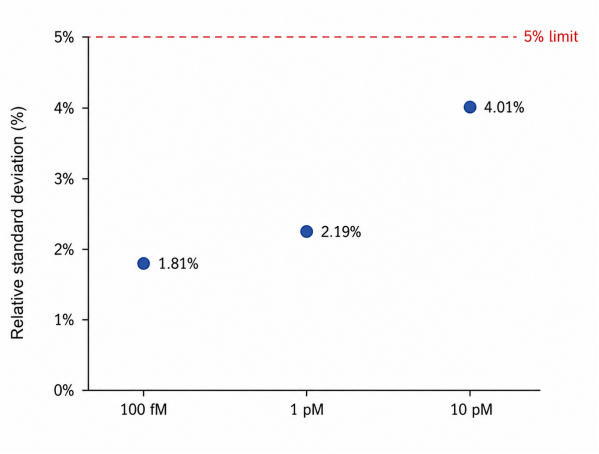

Figure 7: Precision by spike level.

rather than instrument noise.

3.5. Instrumental and matrix interpretation

The presented serum measurements fit the expected behaviour of a nanoporous-gold nucleic-acid biosensor. Immobilization of probe in the nanoporous gold network is expected to enhance capturing probability and electrochemical interaction, though serum remains an analytically challenging medium as proteins, salts, vesicular material, and endogenous nucleic acids might affect target accessibility. Still, the recovered concentration values indicate that these matrix effects could be controlled successfully.

The signed bias results reveal another important analytical detail: slight negative bias in the lowest concentration might be explained by its strong dependency on the blank value, whereas positive biases at higher levels could be caused by various processes such as calibration slope, surface enrichment, signal enhancement effect, and even target concentration dependence. While none of these can be distinguished based on the existing number record, the positive biases did not go beyond acceptable limits.

3.6. Bioanalytical meaning for NSCLC-oriented serum testing

It is important to note that these serum measurement results are relevant only in a specific bioanalytical context. That is, the current data are not sufficient to demonstrate diagnostic utility or patient performance in terms of diagnostic sensitivity, specificity, patient classification, or treatment responsiveness. Instead, they show that the addition of the known amount of miR-18a in serum can be recovered with acceptable accuracy and repeatability using the nanoporous-gold biosensor.

Low-concentration measurement in particular requires special attention. While a serum blank of 24.165 fmol L^{-1} might be neglected in the presence of 10 pmol L^{-1} spike concentration, it constitutes a substantial portion of a 100 fmol L^{-1} concentration. Screening application of this biosensor must thus involve serum blank evaluation, serum pool testing, independent replicate measurements, inter-batch electrode evaluation, and qRT-PCR or digital PCR comparison.

The interpretation map visualizes the recovery results into three analytical zones. The lowest spike concentration 100 fmol L^{-1} falls into the acceptable-but-blank-sensitive category, the middle 1 pmol L^{-1} concentration provides the best stability in terms of blank and signal recovery, while the highest 10 pmol L^{-1} spike concentration is acceptable but upper-bound-near. Thus, this map directly answers the research question in terms of spike concentration reliability.

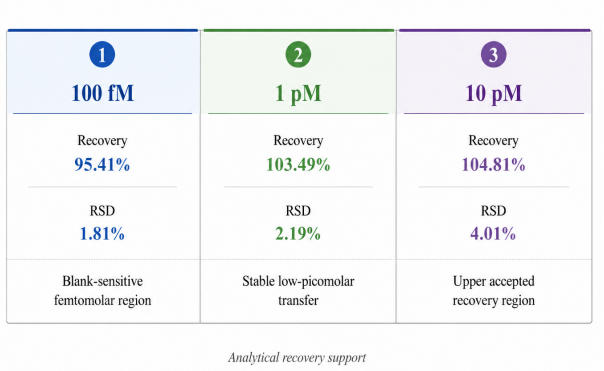

Figure 8: Analytical interpretation map.

4. Conclusion

The obtained data have answered the research question regarding partitioning the endogenous serum blank and measuring its effect on spiked-recovery analysis. Specifically, blank-partitioning procedure turned serum miR-18a recovery measurements at 100 fmol L^{-1}, 1 pmol L^{-1}, and 10 pmol L^{-1} spike concentrations into the concentration-specific interpretation map. Such an answer is far more valuable than merely showing acceptability – it shows where endogenous blank dominates and where added-target recovery is crucial.

The used nanoporous-gold Y-shaped electrochemical biosensor supported the detection of added serum miR-18a at these spike concentrations, with concentrations of 95.415 fmol L^{-1}, 1034.945 fmol L^{-1}, and 10480.525 fmol L^{-1} resulting in recovery of 95.41%, 103.49%, and 104.81%, respectively, with all relative standard deviations below 5%.

The specific answer to the research question is thus that the current serum measurements suggest applicability of the biosensor for serum miR-18a detection within the tested concentration interval. However, the 100 fmol L^{-1} condition represents a critical low-concentration spike point in terms of high blank percentage. The 1 pmol L^{-1} condition represents the best point in terms of low blank contribution and low recovery variability.

References

[1] Mitchell, P. S., Parkin, R. K., Kroh, E. M., Fritz, B. R., Wyman, S. K., Pogosova-Agadjanyan, E. L., . . . & Tewari, M. (2008). Circulating microRNAs as stable blood-based markers for cancer detection. *Proceedings of the National Academy of Sciences, 105*(30), 10513–10518.

[2] Chen, X., Ba, Y., Ma, L., Cai, X., Yin, Y., Wang, K., . . . & Zhang, C. Y. (2008). Characterization of microRNAs in serum: A novel class of biomarkers for diagnosis of cancer and other diseases. *Cell Research, 18*(10), 997–1006.

[3] Bartel, D. P. (2004). MicroRNAs: Genomics, biogenesis, mechanism, and function. *Cell, 116*(2), 281–297.

[4] Leng, Q., Lin, Y., Jiang, F., Lee, C. J., Zhan, M., Fang, H., . . . & Jiang, F. (2017). A plasma miRNA signature for lung cancer early detection. *Oncotarget, 8*(67), 111902.

[5] Ying, L., Du, L., Zou, R., Shi, L., Zhang, N., Jin, J., . . . & Su, D. (2020). Development of a serum miRNA panel for detection of early stage non-small cell lung cancer. *Proceedings of the National Academy of Sciences, 117*(40), 25036–25042.

[6] Gayosso-Gómez, L. V., & Ortiz-Quintero, B. (2021). Circulating microRNAs in blood and other body fluids as biomarkers for diagnosis, prognosis, and therapy response in lung cancer. *Diagnostics, 11*(3), 421.

[7] Komatsu, S., Ichikawa, D., Takeshita, H., Morimura, R., Hirajima, S., Tsujiura, M., . . . & Otsuji, E. (2014). Circulating miR-18a: A sensitive cancer screening biomarker in human cancer. *In Vivo, 28*(3), 293–297.

[8] Shen, K., Cao, Z., Zhu, R., You, L., & Zhang, T. (2019). The dual functional role of microRNA-18a (miR-18a) in cancer development. *Clinical and Translational Medicine, 8*(1), 32.

[9] Kolenda, T., Guglas, K., Kopczyńska, M., Sobocińska, J., Teresiak, A., Bliźniak, R., & Lamperska, K. (2020). Good or not good: Role of miR-18a in cancer biology. *Reports of Practical Oncology and Radiotherapy, 25*(5), 808–819.

[10] Shao, L., Lu, X., Zhou, Y., Wang, Y., Wang, X., Zhuang, Z., & Gong, J. (2021). Altered miR-93-5p/miR-18a expression in serum for diagnosing non-small cell lung cancer. *American Journal of Translational Research, 13*(5), 5073.

[11] Shen, Z., Wu, X., Wang, Z., Li, B., & Zhu, X. (2015). Effect of miR-18a overexpression on the radiosensitivity of non-small cell lung cancer. *International Journal of Clinical and Experimental Pathology, 8*(1), 643.

[12] Labib, M., Khan, N., Ghobadloo, S. M., Cheng, J., Pezacki, J. P., & Berezovski, M. V. (2013). Three-mode electrochemical sensing of ultralow microRNA levels. *Journal of the American Chemical Society, 135*(8), 3027–3038.

[13] Labib, M., & Berezovski, M. V. (2015). Electrochemical sensing of microRNAs: Avenues and paradigms. *Biosensors and Bioelectronics, 68*, 83–94.

[14] El Aamri, M., Yammouri, G., Mohammadi, H., Amine, A., & Korri-Youssoufi, H. (2020). Electrochemical biosensors for detection of microRNA as a cancer biomarker: Pros and cons. *Biosensors, 10*(11), 186.

[15] D'Agata, R., & Spoto, G. (2019). Advanced methods for microRNA biosensing: A problem-solving perspective. *Analytical and Bioanalytical Chemistry, 411*(19), 4425.

[16] Low, S. S., Ji, D., Chai, W. S., Liu, J., Khoo, K. S., Salmanpour, S., . . . & Show, P. L. (2021). Recent progress in nanomaterials modified electrochemical biosensors for the detection of microRNA. *Micromachines, 12*(11), 1409.

[17] Thapa, K., Liu, W., & Wang, R. (2022). Nucleic acid-based electrochemical biosensor: Recent advances in probe immobilization and signal amplification strategies. *Wiley Interdisciplinary Reviews: Nanomedicine and Nanobiotechnology, 14*(1), e1765.

[18] Yu, F., Wang, Y., Yu, C., Zhang, W., & Bai, X. (2024). Sensitive and specific Y-shaped ratio biosensor for detecting serum miR-18a: Potential early scanning tool for non-small cell lung cancer. *Journal of Analysis and Testing, 8*(2), 237–244.